RESEARCH ARTICLE SUMMARY

MOSQUITO GENOMICS

Extensive introgression in a malaria vector species complex revealed by phylogenomics

Michael C. Fontaine,* James B. Pease,* Aaron Steele, Robert M. Waterhouse, Daniel E. Neafsey, Igor V. Sharakhov, Xiaofang Jiang, Andrew B. Hall, Flaminia Catteruccia, Evdoxia Kakani, Sara N. Mitchell, Yi-Chieh Wu, Hilary A. Smith, R. Rebecca Love, Mara K. Lawniczak, Michel A. Slotman, Scott J. Emrich, Matthew W. Hahn,† Nora J. Besansky†

INTRODUCTION: The notion that species boundaries can be porous to introgression is increasingly accepted. Yet the broader role of introgression in evolution remains contentious and poorly documented, partly because of the challenges involved in accurately identifying introgression in the very groups where it is most likely to occur. Recently diverged species often have incomplete reproductive barriers and may hybridize where they overlap. However, because of retention and stochastic sorting of ancestral polymorphisms, inference of the correct species branching order is notoriously challenging for recent speciation events, especially those closely spaced in time. Without knowledge of species relationships, it is impossible to identify instances of introgression.

RATIONALE: Since the discovery that the single mosquito taxon described in 1902 as *Anopheles gambiae* was actually a complex of several closely related and morphologically indistinguishable sibling species, the correct species branching order has remained controversial and unresolved. This Afrotropical complex contains the world's most important vectors of human malaria, owing to their close association with humans, as well as minor vectors and species that do not bite humans. On the basis of ecology and behavior, one might predict phylogenetic clustering of the three highly anthropophilic vector species. However, previous phylogenetic analyses of the complex based on a limited number of markers strongly disagree about relationships between the major vectors, potentially because of historical introgression between them. To investigate the history of the species complex, we used whole-genome reference assemblies, as well as dozens of resequenced individuals from the field.

RESULTS: We observed a large amount of phylogenetic discordance between trees generated from the autosomes and X chromosome. The autosomes, which make up the majority of the genome, overwhelmingly supported the grouping of the three major vectors of malaria, *An. gambiae*, *An. coluzzii*, and *An. arabiensis*. In stark contrast, the X chromosome strongly supported the grouping of *An. arabiensis* with a species that plays no role in malaria transmission, *An. quadriannulatus*. Although the whole-genome consensus phylogeny unequivocally agrees with the autosomal topology, we found that the topology most often located on the X chromosome follows the historical species branching order, with pervasive introgression on the autosomes producing relationships that group the three highly anthropophilic species together. With knowledge of the correct species branching order, we are further able to uncover introgression between another species pair, as well as a complex history of balancing selection, introgression, and local adaptation of a large autosomal inversion that confers aridity tolerance.

CONCLUSION: We identify the correct species branching order of the *An. gambiae* species complex, resolving a contentious phylogeny. Notably, lineages leading to the principal vectors of human malaria were among the first in the complex to radiate and are not most closely related to each other. Pervasive autosomal introgression between these human malaria vectors, including nonsister vector species, suggests that traits enhancing vectorial capacity can be acquired not only through de novo mutation but also through a more rapid process of interspecific genetic exchange.

ON OUR WEB SITE

Read the full article at http://dx.doi.org/10.1126/science.1258524

Time-lapse photographs of an adult anopheline mosquito emerging from its pupal case.

PHOTO CREDIT: JAMES GATHANY, CENTERS FOR DISEASE CONTROL AND PREVENTION

RELATED ITEMS IN *SCIENCE*

D. E. Neafsey *et al.*, *Science* **347**, 1258522 (2015)
DOI: 10.1126/science.1258522

The list of author affiliations is available in the full article online.
*These authors contributed equally to this work.
†Corresponding author. E-mail: mwh@indiana.edu (M.W.H.); nbesansk@nd.edu (N.J.B.)
Cite this article as M. C. Fontaine *et al.*, *Science* **347**, 1258524 (2015). DOI: 10.1126/science.1258524

Downloaded from www.sciencemag.org on January 7, 2015

RESEARCH ARTICLE

MOSQUITO GENOMICS

Extensive introgression in a malaria vector species complex revealed by phylogenomics

Michael C. Fontaine,[1,2]*† James B. Pease,[3]* Aaron Steele,[4] Robert M. Waterhouse,[5,6,7,8] Daniel E. Neafsey,[6] Igor V. Sharakhov,[9,10] Xiaofang Jiang,[10] Andrew B. Hall,[10] Flaminia Catteruccia,[11,12] Evdoxia Kakani,[11,12] Sara N. Mitchell,[11] Yi-Chieh Wu,[5] Hilary A. Smith,[1,2] R. Rebecca Love,[1,2] Mara K. Lawniczak,[13]‡ Michel A. Slotman,[14] Scott J. Emrich,[2,4] Matthew W. Hahn,[3,15]§ Nora J. Besansky[1,2]§

Introgressive hybridization is now recognized as a widespread phenomenon, but its role in evolution remains contested. Here, we use newly available reference genome assemblies to investigate phylogenetic relationships and introgression in a medically important group of Afrotropical mosquito sibling species. We have identified the correct species branching order to resolve a contentious phylogeny and show that lineages leading to the principal vectors of human malaria were among the first to split. Pervasive autosomal introgression between these malaria vectors means that only a small fraction of the genome, mainly on the X chromosome, has not crossed species boundaries. Our results suggest that traits enhancing vectorial capacity may be gained through interspecific gene flow, including between nonsister species.

The notion that species boundaries can be porous to introgression is increasingly accepted. Charismatic cases, such as gene flow between Neanderthals and anatomically modern humans (*1*) or between *Heliconius* butterflies (*2*, *3*), show that introgression can transfer beneficial alleles between closely related species. Yet the broader role of introgression in evolution remains contentious and poorly documented, partly because of the challenges involved in accurately identifying introgression in the very groups where it is most likely to occur. Recently diverged species often have incomplete reproductive barriers, hence, may hybridize in sympatry. However, another feature of rapid radiations is that ancestral polymorphism predating lineage splitting may be sorted stochastically among descendant lineages in a process known as incomplete lineage sorting (ILS). Alleles shared through ILS can be difficult to distinguish from those shared through secondary contact and introgression. Newly developed methods can differentiate these two processes (*1*, *4*) but only if the correct species branching order is known. Because both introgression and ILS cause discordance between gene trees and the species tree, inference of the correct species phylogeny (i.e., the historical branching order of the taxa) is notoriously challenging for recent radiations (*5*–*7*).

Since the discovery that the single mosquito taxon described in 1902 as *Anopheles gambiae* (*8*) was actually a complex of several closely related and morphologically indistinguishable sibling species (known as the *An. gambiae* complex) (*9*), the correct species branching order has remained controversial and unresolved. This Afrotropical complex (*10*–*13*) contains three widely distributed and extensively sympatric species that rank among the world's most important vectors of human malaria, owing to their association with humans (*An. gambiae sensu stricto*, its closest relative and sister species, *Anopheles coluzzii*, and *Anopheles arabiensis*) (Fig. 1A). *Anopheles merus* and *Anopheles melas*, salt-tolerant species that breed in brackish coastal waters of eastern and western Africa, respectively, are minor vectors. *Anopheles quadriannulatus* plays no role in malaria transmission despite vector competence for *Plasmodium falciparum*, as it tends to bite animals other than humans. On the basis of ecology and behavior, one might predict phylogenetic clustering of the highly anthropophilic vector species. Yet such clustering has not been supported by chromosomal inversion phylogenies (*10*, *14*). The apparent phylogenetic affinity between *An. arabiensis* and *An. gambiae* supported by molecular markers and shared chromosomal inversion polymorphisms was instead attributed to introgression (*15*, *16*). Introgression is plausible between any geographically overlapping pair of species in the complex, as reproductive isolation is incomplete: Adult female F_1 hybrids—although uncommon in nature—are fertile and vigorous (only F_1 hybrid males are sterile) (*10*). Nonetheless, comprehensive evidence for introgression between *An. arabiensis* and the other major vector lineage (*An. gambiae* + *An. coluzzii*) has been lacking, until now, because of insufficient genomic resources.

Important malaria vectors make up a small fraction of the genus *Anopheles* but almost invariably are embedded in species complexes similar to that of *An. gambiae sensu lato* (*17*). Thus, resolving the phylogeny of the *An. gambiae* complex has the potential to yield insights into the origin and evolution of traits that are associated with highly successful malaria vectors across the genus as a whole. Here, we have used newly available whole-genome reference assemblies (*18*) to infer the species phylogeny. We found that the two most important malaria vector lineages in the complex are not the most closely related, and we have uncovered pervasive introgression between them. The extent of introgression is such that the phylogenetic tree inferred from whole-genome alignments supports the incorrect species branching order with high confidence.

The X chromosome reflects the species branching order

As a first step in phylogenomic analysis, alignments were generated for existing (*19*, *20*) and newly available genome assemblies, representing six species of the *An. gambiae* complex and two Pyretophorus out-group species (*An. christyi* and *An. epiroticus*) (supplementary text S1 and fig. S1) (*21*). Among the in-group species, the alignment included ~60% of nongap and nonmasked base pairs of the *An. gambiae* PEST reference assembly. Across all assemblies, the proportion of aligned base pairs was lower (~53%) but, nevertheless, spanned more than 93 megabase pairs (Mb) (~40% of the euchromatic genome).

As the *An. gambiae* complex reference genomes were assembled from laboratory colony–derived sequencing template [except for *An. melas* (*18*)], we also performed whole-genome shotgun sequencing of individual field-collected specimens sampled from at least one population of each of the six in-group species (supplementary text S2). Sequencing reads were aligned to the

[1]Department of Biological Sciences, University of Notre Dame, Notre Dame, IN 46556, USA. [2]Eck Institute for Global Health, University of Notre Dame, Notre Dame, IN 46556, USA. [3]Department of Biology, Indiana University, Bloomington, IN 47405, USA. [4]Department of Computer Science and Engineering, University of Notre Dame, Notre Dame, IN 46556, USA. [5]Computer Science and Artificial Intelligence Laboratory, Massachusetts Institute of Technology, 32 Vassar Street, Cambridge, MA 02139, USA. [6]The Broad Institute of MIT and Harvard, 415 Main Street, Cambridge, MA 02142, USA. [7]Department of Genetic Medicine and Development, University of Geneva Medical School, rue Michel-Servet 1, 1211 Geneva, Switzerland. [8]Swiss Institute of Bioinformatics, rue Michel-Servet 1, 1211 Geneva, Switzerland. [9]Department of Entomology, Virginia Polytechnic Institute and State University, Blacksburg, VA 24061, USA. [10]The Interdisciplinary PhD Program in Genetics, Bioinformatics, and Computational Biology, Virginia Polytechnic Institute and State University, Blacksburg, VA 24061, USA. [11]Department of Immunology and Infectious Diseases, Harvard School of Public Health, Boston, MA 02115, USA. [12]Dipartimento di Medicina Sperimentale e Scienze Biochimiche, Università degli Studi di Perugia, Perugia, Italy. [13]Department of Life Sciences, Imperial College London, South Kensington Campus, London SW7 2AZ, UK. [14]Department of Entomology, Texas A&M University, College Station, TX 77843, USA [15]School of Informatics and Computing, Indiana University, Bloomington, IN 47405, USA.
*These authors contributed equally to this work. †Present address: Centre for Ecological and Evolutionary Studies (MarECon group), University of Groningen, Nijenborgh 7, 9747 AG Groningen, Netherlands. ‡Present address: Wellcome Trust Sanger Institute, Hinxton, Cambridge CB10 1SA, UK. **§Corresponding author.**
E-mail: mwh@indiana.edu (M.W.H.); nbesansk@nd.edu (N.J.B.)

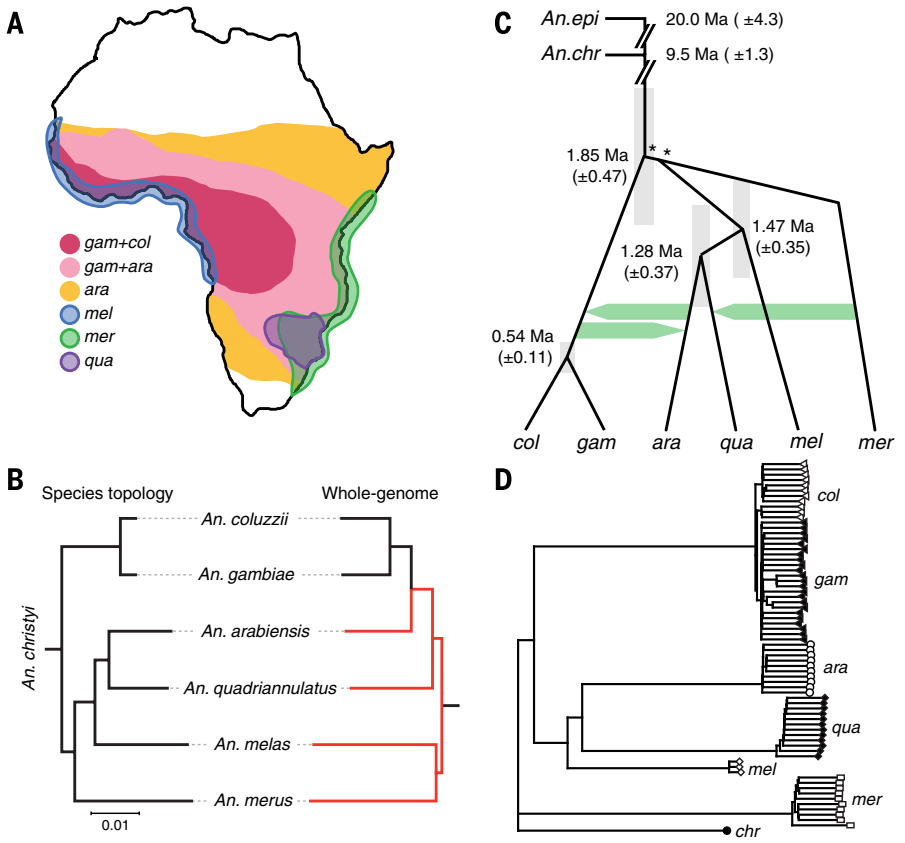

Fig. 1. Distribution and phylogenetic relationships of sequenced members of the *An. gambiae* complex. (**A**) Schematic geographic distribution of *An. gambiae* (gam, formerly *An. gambiae* S form), *An. coluzzii* [col, formerly *An. gambiae* M form (13)], *An. arabiensis* (ara), *An. quadriannulatus* (qua), *An. merus* (mer), and *An. melas* (mel). (**B**) Species topology as estimated from a ML phylogeny of the X chromosome (see text) compared with the ML phylogeny estimated from the whole-genome sequence alignment. The scale-bar denotes nucleotide divergence as calculated by RAxML. Red branches of the latter tree highlight topological differences with the species tree. (**C**) Schematic of the species topology rooted by *An. christyi* (*An. chr*) and *An. epiroticus* (*An. epi*), showing the major introgression events (green arrows) and the approximate divergence and introgression times [Ma ± 1 standard deviation (SD)], if one assumes a substitution rate of 1.1×10^{-9} per site, per generation, and 10 generations per year. The gray bar surrounding each node shows ±2 SD. Nodes marked by asterisks are not fully resolved owing to high levels of ILS. (**D**) Neighbor-joining tree displaying the Euclidian distance between individuals from population samples of each species, calculated using sequence data from the X chromosome. Each species is represented by a distinct symbol shape or shade.

species-appropriate reference assembly to avoid considerable interspecific mapping bias (supplementary text S2, figs. S3 to S4, and table S3), and single-nucleotide variant positions were converted to a common coordinate system relative to the reference genome alignment (supplementary texts S2 and S3 and fig. S2). The results presented below are based on the field-collected samples, but analyses were performed in parallel on the reference genome assemblies, and our findings were consistent in all cases.

To infer the correct species branching order in the face of anticipated ILS and introgression, maximum-likelihood (ML) phylogenies were constructed from 50-kilobase (kb) nonoverlapping windows across the alignments (referred to here as "gene trees" regardless of their protein-coding content), considering six in-group species rooted alternatively with *An. christyi* or *An. epiroticus* (n = 4063 windows) (supplementary text S3). As the choice of out-group did not materially alter our results, we present our findings based on the more closely related species, *An. christyi*. When the 85 tree topologies observed at least once across the genome were sorted by chromosome arm and relative frequency, the most commonly observed trees were strongly discordant between the X chromosome and the autosomes (Fig. 2, table S9, and fig. S16). Although weak disagreement among tree topologies concerning the branching order of basal nodes was a consequence of poor resolution due to ILS (Fig. 1C and fig. S16B), the striking discordance between the X chromosome and the autosomes was not a trivial consequence of lack of phylogenetic signal; conflicting topologies had strong bootstrap support (fig. S16B). Because the major disagreement between the X chromosome and the autosomes concerned the relative phylogenetic positions of *An. arabiensis* and *An. quadriannulatus*, for simplicity, we grouped the most frequently observed topologies into three sets (Fig. 2 and fig. S16), (i) A+CG: those that supported *An. arabiensis* clustering with *An. coluzzii* + *An. gambiae*; (ii) A+CG, R+Q: those that supported both *An. arabiensis* (*An. coluzzii* + *An. gambiae*) and *An. merus* + *An. quadriannulatus*; and (iii) A+Q: those that supported the clustering of *An. arabiensis* and *An. quadriannulatus*. On the X chromosome, all three of the most frequently observed topologies (inferred from 64% of windows) strongly supported the relationship [*melas* (*arabiensis*, *quadriannulatus*)], which indicated a sister-taxon relationship between *An. arabiensis* and *An. quadriannulatus* (i.e., A+Q) (orange shades in Fig. 2). This relationship was shared among all field-collected samples (Fig. 1D). Notably, the X chromosomal windows supporting these topologies are concentrated distal to the centromere (Fig. 3D and supplementary text S3), in an ~15-Mb region corresponding to the Xag inversion whose orientation is ancestral to the *An. gambiae* complex and shared by *An. gambiae*, *An. coluzzii*, and *An. merus* (see supplementary text S5).

In stark contrast to the X chromosome, the overwhelming majority of window-based topologies across the autosomes supported *An. arabiensis* as sister to *An. gambiae* + *An. coluzzii* (green and purple shades in Fig. 2). On chromosomes 3 and 2R, a subset of these topologies also supported a sister-taxon relationship between *An. quadriannulatus* and *An. merus*, in further disagreement with the X chromosome (purple shades, Fig. 2).

Autosomal introgression between *An. arabiensis* and the ancestor of *An. gambiae* + *An. coluzzii* has long been postulated (10, 22) and could explain the strong discordance between the dominant tree topologies of the X and autosomes. However, before this study, the correct species branching order was unresolved, which precluded definitive interpretation of these conflicting signals. To infer the correct historical branching order, we applied a strategy based on sequence divergence (supplementary text S3 and fig. S16). Because introgression will reduce sequence divergence between the species exchanging genes, we expect that the correct species branching order revealed by gene trees constructed from nonintrogressed sequences will show deeper divergences than those constructed from introgressed sequences. If the hypothesis of autosomal introgression is correct, this implies that the topologies supported by the X chromosome should show significantly higher divergence times between *An. arabiensis* and either *An. gambiae* or *An. coluzzii* than topologies supported by the autosomes.

To test this hypothesis, we used *An. arabiensis*, *An. gambiae*, and *An. melas*, as these three species show strongly discordant trees on the X and autosomes. For this trio, there are three possible phylogenetic relationships and two divergence times for each, T_1 and T_2 (Fig. 3A). Using the metrics T_1 and T_2, we conducted two different tests. Initially,

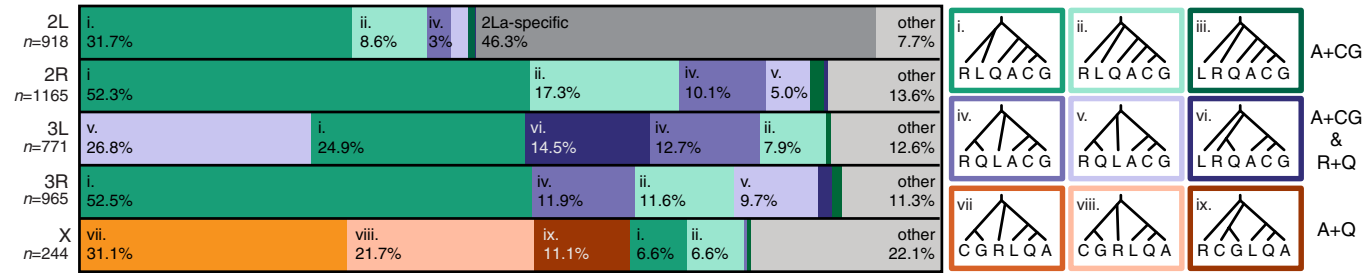

Fig. 2. Phylogenies inferred from regions on the autosomes differ strongly from phylogenies inferred from regions on the X chromosome. ML-rooted phylogenies were inferred from n = 4063 50-kb genomic windows for *An. arabiensis* (A), *An. coluzzii* (C), *An. gambiae* (G), *An. melas* (L), *An. merus* (R), and *An. quadriannulatus* (Q), with *An. christyi* as out-group. The nine most commonly observed topologies across the genome (trees i to ix) are indicated on each of the five chromosome arms (if found) by correspondingly colored blocks whose length represents the proportion of all 50-kb windows on that arm that support the topology. Topologies specific to 2La are represented by the dark gray block on 2L; all other topologies observed on each chromosome arm were pooled, and their combined frequencies are indicated by the light gray blocks. The X chromosome most often indicates that A and Q are sister taxa (trees vii to ix), whereas the autosomes indicate that A and C+G are sister groups (trees i to vi). Large portions of the autosomes (particularly 3L and 3R) indicate that R and Q are sister taxa (trees iv to vi). Additional diversity in inferred trees is the result of rearrangement of three groups (R, C+G, and L+A+Q) because of ILS. The most common phylogeny on the X chromosome (vii) represents the most likely species branching order. The 2L arm has a markedly different distribution of phylogenies because of the unique history of the 2La inversion region (see Fig. 5), which creates unusual phylogenetic topologies found nowhere else in the genome. The autosome-like trees on the X chromosome (i and ii) are entirely found in the pericentromeric region (15 to 24 Mb) (see Fig. 3D), where introgression between *An. arabiensis* and *An. gambiae* + *An. coluzzi* has previously been implicated.

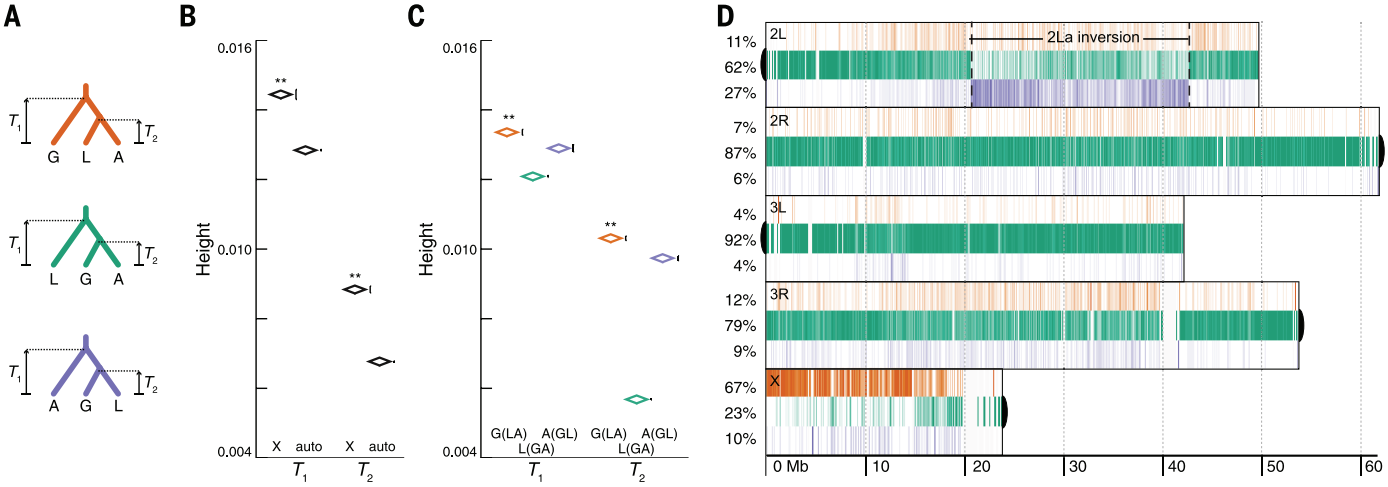

Fig. 3. Tree height reveals the true species branching order in the face of introgression. (**A**) Color-coded trees show the three possible rooted phylogenetic relationships for *An. arabiensis* (A), *An. gambiae s.s.* (G), and *An. melas* (L), with out-group *An. christyi*. For any group of three taxa, there are two species divergence times (T_1 and T_2). When introgression has occurred, a strong decrease is expected in these divergence times. (**B**) Trees on the X chromosome have significantly higher mean values of T_1 and T_2 than the autosomes, which indicates that introgression is more likely to have occurred on the autosomes than the X chromosome (diamond for mean, whiskers ± SEM offset to the right for visual clarity; $^{**}P < 1.0 \times 10^{-40}$). (**C**) Even among only autosomal loci, regions with the X majority relationship G(LA) (orange) have significantly higher T_1 and T_2 ($^{**}P < 1.0 \times 10^{-40}$), which indicates that the autosomal majority topology (green) is the result of widespread introgression between *An. arabiensis* and *An. gambiae*. The X majority relationship G(LA) therefore represents the true species branching relationships. (**D**) The gene tree distributions or "chromoplots" for all five chromosomal arms show that the autosomal and X chromosome phylogenies strongly disagree. Three-taxon phylogenies were inferred from 10-kb chromosomal windows across the genome, and colored vertical bars represent the relative abundance of the three alternative topologies (A) in a 200-kb window. The proportions of the three 10-kb gene trees for each chromosome arm (left) indicate that the autosomes all strongly show a closer relationship between *An. gambiae* and *An. arabiensis* (green); the X indicates a closer relationship between *An. arabiensis* and *An. melas* (orange). Black semicircles indicate the location of centromeres.

we compared mean sequence divergence between X chromosome–based versus autosome-based topologies. As predicted, the estimated mean values of T_1 and T_2 for trees inferred from 10-kb windows on the X chromosome were significantly higher than their counterparts on the autosomes (both $P < 1.0 \times 10^{-40}$) (Fig. 3B). However, the possibility exists that this result was confounded or entirely driven by other factors that differ between the X and autosomes, including a faster rate of evolution on the X (*23*). Indeed, we found evidence supporting faster evolution of genes on the X chromosome (supplementary text S3 and fig. S23). To avoid this problem, we conducted a second test on the autosomes alone, focusing on trees inferred from 10-kb windows and the mean divergence levels among those supporting the three possible phylogenetic relationships illustrated in Fig. 3A. The result, congruent with the first test but providing unequivocal evidence for the correct species branching order, was that the set of autosomal trees supporting the majority X chromosome topology [*gambiae* (*melas*, *arabiensis*)] again had the highest mean values of T_1 and T_2 (both $P < 1.0 \times 10^{-40}$) (Fig. 3C). This indicates that the species branching order inferred from the X chromosome is the correct one (Fig. 1B), despite extensive amounts of *An. gambiae–An. arabiensis* autosomal introgression (Fig. 3D and fig. S16).

The total-evidence approach to phylogenetic reconstruction (*24*) is premised on the notion that the best estimate of species relationships arises

from character congruence when all available data are considered simultaneously. Alternative approaches seek taxonomic congruence between different data sets or data partitions, analyzed separately (25). Either way, standard phylogenomic practice entails some form of "majority rule," based on the assumption that as the amount of data increases so will the probability of converging on the correct species branching order [apart from exceptional cases (26)]. Because of both ILS and introgression, the historical species branching order for the *An. gambiae* complex is represented by only 1.9% of 50-kb windows across the entire genome (Fig. 2). As a result, when we inferred a ML tree for the *An. gambiae* complex on the basis of whole-genome alignments, we recovered the wrong species branching order supported by 100% of the bootstrap replicates at each node (Fig. 1B, supplementary text S3, and figs. S17A and S18A). The extent of autosomal introgression in the *An. gambiae* complex has the paradoxical effect that, as an increasing amount of the genome is sampled, support for the incorrect species branching order is maximized.

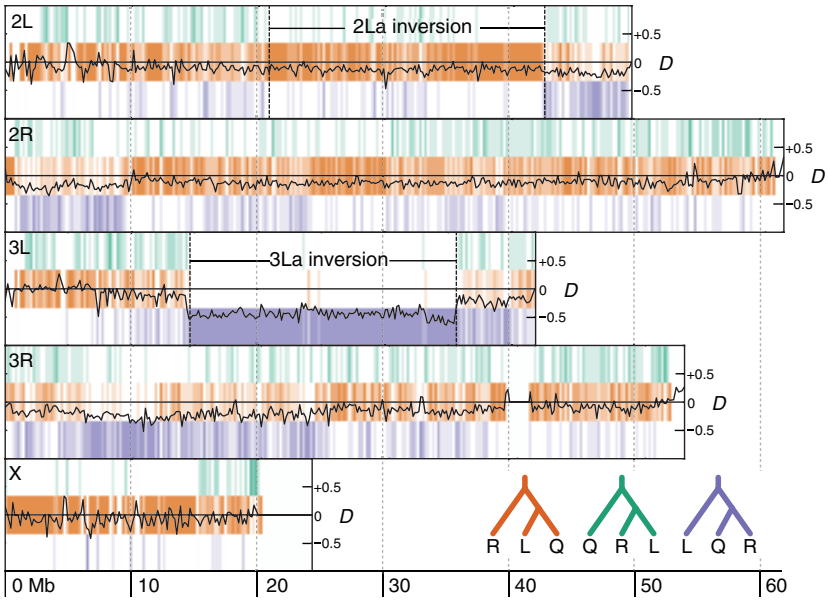

Fig. 4. Introgression between *An. merus* and *An. quadriannulatus*. Chromoplots for all five chromosomal arms show a highly spatially heterogeneous distribution of phylogenies inferred from 50-kb genomic regions, particularly on 3L. The three possible rooted phylogenetic relationships for *An. quadriannulatus* (Q), *An. melas* (L), and *An. merus* (R), with out-group *An. christyi* are shown, colored according to the key in the lower right. The region on 3L corresponding to the 3La inversion shows strong evidence of R-Q introgression and a strong negative deviation of the *D* statistic. The region on 2L corresponding to the 2La inversion is highly enriched for the R(LQ) relationship, as expected, given that L and Q both have the 2L+^{a} orientation, whereas R has 2La (see Fig. 5). Across all the autosomes, the *D* statistic generally trends toward negative values, which indicates weak or ancient R-Q introgression may have been occurring across the autosomes (see supplementary text S3).

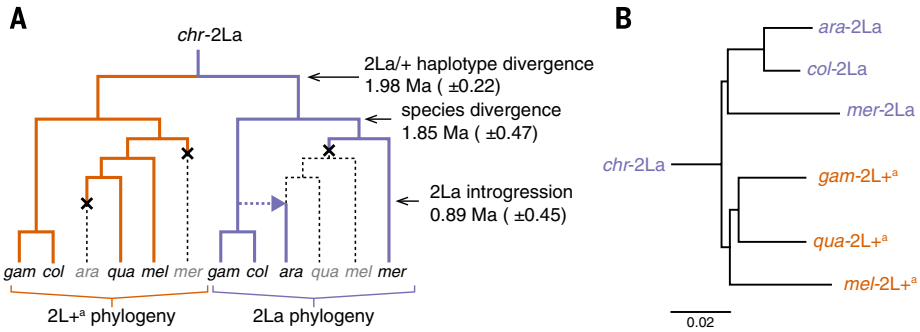

Fig. 5. Ancient trans-specific polymorphism of an inversion predates radiation of the *An. gambiae* complex. (**A**) All species in the complex are fixed for either the 2La (*An. arabiensis*, *ara*; *An. merus*, *mer*) or 2L+^{a} (*An. melas*, *mel*) orientation of the 2La rearrangement except *An. gambiae* (gam) and *An. coluzzii* (col), which remain polymorphic for both orientations. The unique phylogenies observed in the 2La region (Fig. 2) are the result of differential loss (×) of the 2La and 2L+^{a} orientations and the introgression of 2La from the ancestral population of *An. gambiae* + *coluzzii* into *An. arabiensis* (dotted arrow). The overall divergence between the 2La and 2L+^{a} orientations inferred from sequences inside the inversion breakpoints is higher, on average, than the predicted divergence time of the species complex. (**B**) ML phylogeny inferred from sequences of the two different orientations of the 2La region (2La and 2L+^{a}) shows that the divergence between opposite orientations is greater than the divergence between the same orientation present in different species (all nodes, 100% bootstrap support). Particularly notable is the separation of the sister taxa *An. gambiae*-2L+^{a} and *An. coluzzii*-2La, as these are known sister taxa. The scale bar denotes nucleotide divergence as calculated by RAxML.

Autosomal permeability of species boundaries

Early cytotaxonomic evidence (10, 12, 27), as well as more recent ribosomal DNA–based evidence (28, 29), supports rare occurrences (<0.1%) of natural female F_1 hybrids between *An. arabiensis*–*An. gambiae* + *An. coluzzii*, *An. arabiensis*–*An. quadriannulatus*, and *An. melas*–*An. gambiae* + *An. coluzzii*, although there are no reports of hybrids involving *An. merus*. The evolutionary importance of these rare hybrids as bridges to interspecific gene flow has remained controversial. Inference of the correct species branching order for the *An. gambiae* complex (Fig. 1B) allowed a systematic analysis of introgression across the genomes of six members of this complex using the *D* (1, 4) and D_{FOIL} (30) statistics (supplementary text S4).

As expected, such tests revealed pervasive introgression across all autosomes between *An. arabiensis* and the ancestor of *An. gambiae* + *An. coluzzii* (figs. S24 and S25). Although introgression was detected in both directions, the majority involved genetic transfer from *An. arabiensis* into the ancestor of *An. gambiae* + *An. coluzzii*. This recent and massive episode of introgression impedes our ability to detect older introgression events between these species. Unexpectedly, we also found evidence of extensive autosomal introgression between another species pair, *An. merus* and *An. quadriannulatus* (Fig. 4, supplementary text S3, and figs. S24 and S25). One of the most striking of the introgressed regions was a contiguous block of genes coincident with the ~22-Mb 3La chromosomal inversion (31). The corresponding sequence originally present in ancestral populations of *An. quadriannulatus* has been entirely replaced by its counterpart from *An. merus*, a conclusion supported by the clustering of *An. merus* with *An. quadriannulatus* in gene trees constructed from sequences in the 3La inversion (figs. S19, C and D, and S21B). Extant populations of both of these species, and indeed all recognized species in the *An. gambiae* complex, are fixed for the standard (3L+^{a}) orientation except *An. melas* and its putative sister species *An. bwambae*, both fixed for the 3La orientation (31). Considering that the exact ~22-Mb 3La region was replaced between species whose contemporary populations are collinear for 3L+^{a}, it is conceivable that ancestral *An. quadriannulatus* populations originally carried 3La before the 3L+^{a} introgression. The expected reduced recombination between

inverted and standard arrangements in inversion heterozygotes may explain why the introgressed region is coincident with the entire 22-Mb 3La region.

The introgression profile was consistent between samples from natural populations and the reference genome assemblies, involving the same species pairs and the same chromosomal locations (supplementary text S4 and fig. S24). Moreover, based on population samples from multiple geographic locations in Africa, patterns of introgression between *An. arabiensis* and *An. gambiae* + *An. coluzzii*, and between *An. merus* and *An. quadriannulatus*, are similar across their geographic range (fig. S25 and table S10). These findings refute the possibility that introgression was an unnatural artifact of colonization and laboratory maintenance of multiple species. The lack of geographic variation in patterns of introgression also suggests that autosomal introgression occurred sufficiently long ago to have spread across subpopulations. By contrast, mitochondrial DNA (mtDNA) revealed patterns consistent with ongoing gene flow between *An. arabiensis* and *An. gambiae* or *An. coluzzii* (supplementary text 3.3 and fig. S22).

Transspecific inversion polymorphism

The unusually high sequence divergence between alternative orientations of a chromosomal inversion polymorphic within *An. gambiae* and *An. coluzzii* (2La and 2L+^{a}) has been noted previously (*32*, *33*) but has not been adequately explained. Other species in the complex are fixed for either 2La (*An. arabiensis* and *An. merus*) or 2L+^{a} (*An. quadriannulatus* and *An. melas*) (*31*) (Fig. 5A). In *An. gambiae* and *An. coluzzii*, the 2La arrangement has been shown to confer superior resistance to desiccating environments (*34*, *35*) relative to 2L+^{a}, and its frequency correlates with environmental gradients of aridity (*10*, *32*). It has been argued that 2La introgressed from *An. arabiensis* into the presumed 2L+^{a} ancestor of *An. gambiae* + *An. coluzzii* (*36*), a crucial step facilitating the range expansion of a presumed forest-adapted species into drier savannas. Sequence divergence-based estimates of the age of 2La and 2L+^{a} arrangements relative to the age of the species complex (Fig. 1C) suggest a radically different scenario in which 2La/2L+^{a} is an ancient inversion polymorphism that predates the initial diversification of the entire complex but is maintained as polymorphic only in *An. gambiae* and *An. coluzzii* (Fig. 5). Consistent with this scenario, the topology of the gene tree built from sequences inside the inversion boundaries indicates that species are grouped by their 2La or 2L+^{a} karyotype (Fig. 5B). Furthermore, contrary to the longstanding assumption (*36*), our data suggest that 2La introgressed from ancestral *An. gambiae* into *An. arabiensis*, not the other way around—eventually replacing the *An. arabiensis* 2L+^{a} arrangement (Fig. 5A). Our inference about the direction of 2La introgression, as well as the underlying phylogenetic hypothesis for the *An. gambiae* complex, are consistent with the genome-enabled chromosomal inversion phylogeny of the *An. gambiae* complex reconstructed from ancestral and derived gene orders at the breakpoints of 10 fixed chromosomal inversions (supplementary text S5 and fig. S27).

Functional insights from differential genetic exchange

We found that introgression mainly involved the autosomes. Our data suggest that the X chromosome is largely resistant to introgression, consistent with studies in this and other systems indicating that the X (or Z) disproportionately harbors factors responsible for reproductive isolation (*3*, *6*, *37*–*41*). The nature, number, and chromosomal organization of these X-linked factors are unsolved puzzles for future research, but our data offer one tantalizing clue. *An. gambiae* males deliver to females large amounts of 20-hydroxyecdysone (20E) (*42*), a steroid hormone that increases female fertility (*43*) and fecundity (*44*) and regulates mating behavior and success (*45*). The cytochrome p450 gene *CYP315A1* (AGAP000284) that synthesizes the 20E precursor ecdysone is located near the distal end of the X chromosome. Furthermore, this region is associated with male hybrid sterility between *An. gambiae* and *An. arabiensis*, with the *An. gambiae* X chromosome causing inviability in an *An. arabiensis* genetic background (*40*). Combined with our data showing that male *An. arabiensis* produce significantly less 20E than *An. gambiae* (supplementary text S6 and fig. S28), these observations prompt the hypothesis that divergence in 20E function between the two species may have a role in speciation through possible effects on the reproductive fitness of hybrid males.

Pervasive autosomal introgression between *An. arabiensis* and the *An. gambiae*–clade ancestor is consistent with the paucity of sterility factors across much of the autosomes, although several autosomal quantitative trait loci have been mapped in both species (*40*). Accordingly, we explored the small subset of autosomal genes (n = 485) that showed no indication of introgression (supplementary text S6), as these are candidates contributing to reproductive isolation. We found a remarkable overrepresentation of genes encoding cyclic-nucleotide phosphodiesterases, enzymes that regulate the levels of the messengers cyclic adenosine monophosphate and cyclic guanosine monophosphate (*46*), which in turn control (among other processes) ecdysone synthesis (*47*, *48*) (table S16).

Implications for the evolution of vectorial capacity

Initial radiation of the *An. gambiae* complex was both recent and rapid. Counter to the traditional view (*49*), it is now clear that the ancestor of the principal malaria vectors *An. gambiae* and *An. coluzzii* separated from other species in the group approximately 2 million years ago (Ma) and that *An. gambiae* and *An. coluzzii* are distantly related to the other primary vector in the group, *An. arabiensis*. Extant populations of *An. gambiae* and *An. coluzzii* are highly anthropophilic vectors, dependent upon humans for blood meals, adult shelter, and larval breeding sites, yet anthropogenic influences are unlikely to have triggered their cladogenesis an estimated 0.5 Ma. Instead, anthropophilic traits are likely to have developed in conjunction with the expansion of Neolithic human populations that occurred more recently. Despite a history of extensive introgression with *An. arabiensis*, *An. gambiae* and *An. coluzzii* are behaviorally, physiologically, ecologically, and epidemiologically distinct from *An. arabiensis*; the same is true for *An. merus* and *An. quadriannulatus*. Notably, experimental introgressions of certain autosomal inversions result in stable heterotic polymorphisms, whereas other introgressed autosomal and X chromosome inversions are rapidly eliminated (*22*), consistent with a role for natural selection in the fate of introgressed regions. Given evidence that the 2La inversion polymorphism is maintained by selection in *An. gambiae* and *An. coluzzii* (*32*, *50*), it seems likely that its introgression into *An. arabiensis* was adaptive, and bidirectional introgressions across the genome between these species probably contributed to their wide ecological flexibility and their vectorial capacity. Broad overlap exists between geographic ranges of these species, and the potential for ongoing hybridization and introgression remains, including the opportunity for introgression of insecticide resistance alleles (*51*). Our study establishes a foundation for further study of adaptive introgression in this species complex and its role in shaping vectorial capacity in this and other malaria vector species complexes.

REFERENCES AND NOTES

1. R. E. Green *et al.*, A draft sequence of the Neandertal genome. *Science* **328**, 710–722 (2010). doi: 10.1126/science.1188021; pmid: 20448178
2. K. K. Dasmahapatra *et al.*, Butterfly genome reveals promiscuous exchange of mimicry adaptations among species. *Nature* **487**, 94–98 (2012). doi: 10.1038/nature11041; pmid: 22722851
3. S. H. Martin *et al.*, Genome-wide evidence for speciation with gene flow in *Heliconius* butterflies. *Genome Res.* **23**, 1817–1828 (2013). doi: 10.1101/gr.159426.113; pmid: 24045163
4. E. Y. Durand, N. Patterson, D. Reich, M. Slatkin, Testing for ancient admixture between closely related populations. *Mol. Biol. Evol.* **28**, 2239–2252 (2011). doi: 10.1093/molbev/msr048; pmid: 21325092
5. D. Garrigan *et al.*, Genome sequencing reveals complex speciation in the *Drosophila simulans* clade. *Genome Res.* **22**, 1499–1511 (2012). doi: 10.1101/gr.130922.111; pmid: 22534282
6. M. A. White, C. Ané, C. N. Dewey, B. R. Larget, B. A. Payseur, Fine-scale phylogenetic discordance across the house mouse genome. *PLOS Genet.* **5**, e1000729 (2009). doi: 10.1371/journal.pgen.1000729; pmid: 19936022
7. N. Patterson, D. J. Richter, S. Gnerre, E. S. Lander, D. Reich, Genetic evidence for complex speciation of humans and chimpanzees. *Nature* **441**, 1103–1108 (2006). doi: 10.1038/nature04789; pmid: 16710306
8. G. M. Giles, *A handbook of the gnats or mosquitoes giving the anatomy and life history of the Culicidae together with descriptions of all species noticed up to the present date*. (John Bale, Sons & Danielsson, Ltd., London, 1902).
9. G. Davidson, *Anopheles gambiae* complex. *Nature* **196**, 907 (1962). doi: 10.1038/196907a0
10. M. Coluzzi, A. Sabatini, V. Petrarca, M. A. Di Deco, Chromosomal differentiation and adaptation to human environments in the *Anopheles gambiae* complex. *Trans. R. Soc. Trop. Med. Hyg.* **73**, 483–497 (1979). doi: 10.1016/0035-9203(79)90036-1; pmid: 394408
11. B. J. White, F. H. Collins, N. J. Besansky, Evolution of *Anopheles gambiae* in relation to humans and malaria. *Annu. Rev. Ecol. Evol. Syst.* **42**, 111–132 (2011). doi: 10.1146/annurev-ecolsys-102710-145028

12. G. B. White, *Anopheles gambiae* complex and disease transmission in Africa. *Trans. R. Soc. Trop. Med. Hyg.* **68**, 278–301 (1974). doi: 10.1016/0035-9203(74)90035-2; pmid: 4420769
13. M. Coetzee *et al*., *Anopheles coluzzii* and *Anopheles amharicus*, new members of the *Anopheles gambiae* complex. *Zootaxa* **3619**, 246–274 (2013). doi: 10.11646/zootaxa.3619.3.2
14. N. J. Besansky *et al*., Molecular phylogeny of the *Anopheles gambiae* complex suggests genetic introgression between principal malaria vectors. *Proc. Natl. Acad. Sci. U.S.A.* **91**, 6885–6888 (1994). doi: 10.1073/pnas.91.15.6885; pmid: 8041714
15. B. A. García, A. Caccone, K. D. Mathiopoulos, J. R. Powell, Inversion monophyly in African anopheline malaria vectors. *Genetics* **143**, 1313–1320 (1996). pmid: 8807303
16. N. J. Besansky *et al*., Semipermeable species boundaries between *Anopheles gambiae* and *Anopheles arabiensis*: Evidence from multilocus DNA sequence variation. *Proc. Natl. Acad. Sci. U.S.A.* **100**, 10818–10823 (2003). doi: 10.1073/pnas.1434337100; pmid: 12947038
17. R. E. Harbach, in *Anopheles Mosquitoes: New Insights into Malaria Vectors*, S. Manguin, Ed. (InTech, DOI: 10.5772/54695, 2013), chap. 1, pp. 3–55. doi: 10.5772/54695
18. D. E. Neafsey *et al*., *Science* **346**, 10.1126/science.1258522 (2014).
19. R. A. Holt *et al*., The genome sequence of the malaria mosquito *Anopheles gambiae*. *Science* **298**, 129–149 (2002). doi: 10.1126/science.1076181; pmid: 12364791
20. M. K. Lawniczak *et al*., Widespread divergence between incipient *Anopheles gambiae* species revealed by whole genome sequences. *Science* **330**, 512–514 (2010). doi: 10.1126/science.1195755; pmid: 20966253
21. Supplementary text, figures, and tables are available on *Science* Online.
22. A. della Torre, L. Merzagora, J. R. Powell, M. Coluzzi, Selective introgression of paracentric inversions between two sibling species of the *Anopheles gambiae* complex. *Genetics* **146**, 239–244 (1997). pmid: 9136013
23. B. Charlesworth, J. A. Coyne, N. H. Barton, The relative rates of evolution of sex chromosomes and autosomes. *Am. Nat.* **130**, 113–146 (1987). doi: 10.1086/284701
24. D. J. Eernisse, A. G. Kluge, Taxonomic congruence versus total evidence, and amniote phylogeny inferred from fossils, molecules, and morphology. *Mol. Biol. Evol.* **10**, 1170–1195 (1993). pmid: 8277850
25. S. V. Edwards, Is a new and general theory of molecular systematics emerging? *Evolution* **63**, 1–19 (2009). doi: 10.1111/j.1558-5646.2008.00549.x; pmid: 19146594
26. J. H. Degnan, N. A. Rosenberg, Discordance of species trees with their most likely gene trees. *PLOS Genet.* **2**, e68 (2006). doi: 10.1371/journal.pgen.0020068; pmid: 16733550
27. J. H. Bryan, Observations on the member species of the *Anopheles gambiae* complex in The Gambia, West Africa. *Trans. R. Soc. Trop. Med. Hyg.* **73**, 463–466 (1979). doi: 10.1016/0035-9203(79)90179-2; pmid: 555076
28. E. A. Temu, R. H. Hunt, M. Coetzee, J. N. Minjas, C. J. Shiff, Detection of hybrids in natural populations of the *Anopheles gambiae* complex by the rDNA-based, PCR method. *Ann. Trop. Med. Parasitol.* **91**, 963–965 (1997). doi: 10.1080/00034989760383; pmid: 9579219
29. C. Costantini *et al*., Living at the edge: Biogeographic patterns of habitat segregation conform to speciation by niche expansion in *Anopheles gambiae*. *BMC Ecol.* **9**, 16 (2009). doi: 10.1186/1472-6785-9-16; pmid: 19460144
30. J. B. Pease, M. W. Hahn, Detection and polarization of introgression in a five-taxon phylogeny. *BioRxiv* 10.1101/004689 (2014). doi: 10.1101/004689
31. M. Coluzzi, A. Sabatini, A. della Torre, M. A. Di Deco, V. Petrarca, A polytene chromosome analysis of the *Anopheles gambiae* species complex. *Science* **298**, 1415–1418 (2002). doi: 10.1126/science.1077769; pmid: 12364623
32. C. Cheng *et al*., Ecological genomics of *Anopheles gambiae* along a latitudinal cline: A population-resequencing approach. *Genetics* **190**, 1417–1432 (2012). doi: 10.1534/genetics.111.137794; pmid: 22209907
33. B. J. White *et al*., The population genomics of trans-specific inversion polymorphisms in *Anopheles gambiae*. *Genetics* **183**, 275–288 (2009). doi: 10.1534/genetics.109.105817; pmid: 19581444
34. C. Fouet, E. Gray, N. J. Besansky, C. Costantini, Adaptation to aridity in the malaria mosquito *Anopheles gambiae*: Chromosomal inversion polymorphism and body size influence resistance to desiccation. *PLOS ONE* **7**, e34841 (2012). doi: 10.1371/journal.pone.0034841; pmid: 22514674
35. E. M. Gray, K. A. Rocca, C. Costantini, N. J. Besansky, Inversion 2La is associated with enhanced desiccation resistance in *Anopheles gambiae*. *Malar. J.* **8**, 215 (2009). doi: 10.1186/1475-2875-8-215; pmid: 19772577
36. J. R. Powell, V. Petrarca, A. della Torre, A. Caccone, M. Coluzzi, Population structure, speciation, and introgression in the *Anopheles gambiae* complex. *Parassitologia* **41**, 101–113 (1999). pmid: 10697841
37. S. Sankararaman *et al*., The genomic landscape of Neanderthal ancestry in present-day humans. *Nature* **507**, 354–357 (2014). doi: 10.1038/nature12961; pmid: 24476815
38. M. Meyer *et al*., A high-coverage genome sequence from an archaic Denisovan individual. *Science* **338**, 222–226 (2012). doi: 10.1126/science.1224344; pmid: 22936568
39. J. A. Coyne, H. A. Orr, *Speciation* (Sinauer Associates, Sunderland, MA, 2004).
40. M. Slotman, A. Della Torre, J. R. Powell, The genetics of inviability and male sterility in hybrids between *Anopheles gambiae* and *An. arabiensis*. *Genetics* **167**, 275–287 (2004). doi: 10.1534/genetics.167.1.275; pmid: 15166154
41. S. M. O'Loughlin *et al*., Genomic analyses of three malaria vectors reveals extensive shared polymorphism but contrasting population histories. *Mol. Biol. Evol.* **31**, 889–902 (2014). doi: 10.1093/molbev/msu040; pmid: 24408911
42. E. Pondeville, A. Maria, J. C. Jacques, C. Bourgouin, C. Dauphin-Villemant, *Anopheles gambiae* males produce and transfer the vitellogenic steroid hormone 20-hydroxyecdysone to females during mating. *Proc. Natl. Acad. Sci. U.S.A.* **105**, 19631–19636 (2008). doi: 10.1073/pnas.0809264105; pmid: 19060216
43. W. R. Shaw *et al*., Mating activates the heme peroxidase HPX15 in the sperm storage organ to ensure fertility in *Anopheles gambiae*. *Proc. Natl. Acad. Sci. U.S.A.* **111**, 5854–5859 (2014). doi: 10.1073/pnas.1401715111; pmid: 24711401
44. F. Baldini *et al*., The interaction between a sexually transferred steroid hormone and a female protein regulates oogenesis in the malaria mosquito *Anopheles gambiae*. *PLOS Biol.* **11**, e1001695 (2013). doi: 10.1371/journal.pbio.1001695; pmid: 24204210
45. P. Gabrieli *et al*., Sexual transfer of the steroid hormone 20E induces the postmating switch in *Anopheles gambiae*. *Proc. Natl. Acad. Sci. U.S.A.* **111**, 16353–16358 (2014). doi: 10.1073/pnas.1410488111; pmid: 25368171
46. A. T. Bender, J. A. Beavo, Cyclic nucleotide phosphodiesterases: Molecular regulation to clinical use. *Pharmacol. Rev.* **58**, 488–520 (2006). doi: 10.1124/pr.58.3.5; pmid: 16968949
47. B. A. Cooke, Signal transduction involving cyclic AMP-dependent and cyclic AMP-independent mechanisms in the control of steroidogenesis. *Mol. Cell. Endocrinol.* **151**, 25–35 (1999). doi: 10.1016/S0303-7207(98)00255-X; pmid: 10411317
48. G. Manière, E. Vanhems, F. Gautron, J. P. Delbecque, Inhibition of ovarian steroidogenesis by cyclic GMP in a fly. *J. Endocrinol.* **177**, 35–44 (2003). doi: 10.1677/joe.0.1770035; pmid: 12697035
49. F. J. Ayala, M. Coluzzi, Chromosome speciation: Humans, *Drosophila*, and mosquitoes. *Proc. Natl. Acad. Sci. U.S.A.* **102** (suppl. 1), 6535–6542 (2005). doi: 10.1073/pnas.0501847102; pmid: 15851677
50. B. J. White *et al*., Localization of candidate regions maintaining a common polymorphic inversion (2La) in *Anopheles gambiae*. *PLOS Genet.* **3**, e217 (2007). doi: 10.1371/journal.pgen.0030217; pmid: 18069896
51. H. D. Mawejje *et al*., Insecticide resistance monitoring of field-collected *Anopheles gambiae s.l.* populations from Jinja, eastern Uganda, identifies high levels of pyrethroid resistance. *Med. Vet. Entomol.* **27**, 276–283 (2013). doi: 10.1111/j.1365-2915.2012.01055.x; pmid: 23046446

ACKNOWLEDGMENTS

We thank M. Kern and B. J. White for early assistance with this project. Genome assemblies and sequence reads generated by the Broad and the BGI have been submitted to National Center for Biotechnology Information, NIH, under two umbrella BioProject IDs: PRJNA6751 and PRJNA254046. The mitochondrial genome alignments, VCF files of field individual samples, the Multiple Alignment Format *Threaded-Blockset Aligner* (MAF TBA) genome alignment of reference assemblies, and the MAF genome alignment from high depth field samples are available on Dryad: doi:10.5061/dryad.f4114. Sequencing was funded at the Broad Institute by a grant from the National Human Genome Research Institute. Individual laboratories were funded by the NIH [R01AI076584 (N.J.B., M.W.H.), R21AI101459 (N.J.B., H.A.S.), R21AI094289 and R21AI099528 (I.V.S.), R01AI104956 (F.C.), R01AI085079 (M.A.S.), HHSN272200900039C (S.J.E.), T32GM007757 (J.B.P.)], Foundation for the National Institutes of Health through the Vector-based Control of Transmission Discovery Research program of the Grand Challenges in Global Health Initiative (N.J.B., M.C.F.), Marie Curie International Outgoing Fellowship (R.M.W.), Department of Education Graduate Assistance in Areas of National Need fellowship (A.S.), Richard and Peggy Notebaert Premier Fellowship and Jack Kent Cooke Foundation Graduate Scholarship (R.R.L.), Fralin Life Science Institute of Virginia Tech (I.V.S.), U.K. Medical Research Council Career Development Award (M.K.L.), European Research Council FP7 (Starting Grant 260897 to F.C.). Author contributions: conceived project: N.J.B.; coordinated project: N.J.B., M.C.F.; supervised project at the Broad Institute: D.E.N.; genome alignments: R.M.W.; genomic data processing, read mapping, development of pipelines for variant calling and scripts for coordinate conversion, mtDNA genome reconstruction: A.S., M.C.F., S.J.E.; provided access to *An. gambiae* genomic sequences from Mali: R.R.L.; window-based phylogeny reconstruction, development and implementation of chromoplots, development and implementation of divergence-based method to infer species branching order; estimation of sequence-based divergence times: J.B.P., M.W.H.; introgression testing: J.B.P., M.C.F., M.W.H.; polymorphism and divergence analyses, phylogenomic analyses of nuclear and mtDNA genomes: M.C.F.; orthology predictions and gene-based phylogenetic reconstruction: R.M.W., Y.-C.W.; identification of inversion breakpoints, chromosomal inversion phylogeny, estimation of divergence time based on rates of rearrangement: I.V.S., A.B.H., X.J.; genomic library construction, H.A.S., M.C.F.; functional enrichment analyses: H.A.S., M.C.F., J.B.P.; ecdysteroid quantification: F.C., E.K., S.N.M.; molecular evolution: D.E.N., M.K.L., M.A.S.; wrote paper: N.J.B., M.C.F., M.W.H. with input from other authors.

SUPPLEMENTARY MATERIALS

www.sciencemag.org/content/347/6217/1258524/suppl/DC1
Supplementary Text
Figs. S1 to S28
Tables S1 to S16
References (*52*–*110*)

9 July 2014; accepted 14 November 2014
Published online 27 November 2014;
10.1126/science.1258524

EXTENDED PDF SPONSORED
BY BIO-TECHNE.COM
bio-techne
LIFE SCIENCE BRANDS
R&D systems NOVUS BIOLOGICALS TOCRIS
LEARN MORE
http://bio-techne.com/launch/?utm_source=Science.com
&utm_medium=PDF%20banner&utm_campaign=Launchv2

Science
AAAS

Extensive introgression in a malaria vector species complex revealed by phylogenomics

Michael C. Fontaine *et al.*

Science **347**, (2015);
DOI: 10.1126/science.1258524

This copy is for your personal, non-commercial use only.

If you wish to distribute this article to others, you can order high-quality copies for your colleagues, clients, or customers by clicking here.

Permission to republish or repurpose articles or portions of articles can be obtained by following the guidelines here.

The following resources related to this article are available online at www.sciencemag.org (this information is current as of January 7, 2015):

Updated information and services, including high-resolution figures, can be found in the online version of this article at:
http://www.sciencemag.org/content/347/6217/1258524.full.html

Supporting Online Material can be found at:
http://www.sciencemag.org/content/suppl/2014/11/25/science.1258524.DC1.html

A list of selected additional articles on the Science Web sites **related to this article** can be found at:
http://www.sciencemag.org/content/347/6217/1258524.full.html#related

This article **cites 101 articles**, 61 of which can be accessed free:
http://www.sciencemag.org/content/347/6217/1258524.full.html#ref-list-1

This article appears in the following **subject collections:**
Evolution
http://www.sciencemag.org/cgi/collection/evolution

Downloaded from www.sciencemag.org on January 7, 2015

Science (print ISSN 0036-8075; online ISSN 1095-9203) is published weekly, except the last week in December, by the American Association for the Advancement of Science, 1200 New York Avenue NW, Washington, DC 20005. Copyright 2015 by the American Association for the Advancement of Science; all rights reserved. The title *Science* is a registered trademark of AAAS.